

Generation of a double shock driven by laser

A. Benuzzi-Mounaix, M. Koenig, G. Huser, B. Faral, and N. Grandjouan

Laboratoire pour l'Utilisation des Lasers Intenses (LULI), Unité Mixte No. 7605, CNRS, CEA, Ecole Polytechnique, Université Pierre et Marie Curie, 91128 Palaiseau, France

D. Batani, E. Henry, and M. Tomasini

Dipartimento di Fisica "G. Occhialini," Università degli Studi di Milano Bicocca and INFN, Piazza della Scienza 3, 20126 Milano, Italy

T. A. Hall

University of Essex, Colchester CO4 3SQ, United Kingdom

F. Guyot

Laboratoire de Mineralogie-Cristallographie Paris, IPGP Université Paris VI et Paris VII, bat. 7 140 rue de Lourmel 75015 Paris, France

(Received 15 December 2003; published 27 October 2004)

The feasibility and reliability of a multiple laser shock generation to study the equation of state surface off the principal Hugoniot curve and to approach an isentropic compression has been demonstrated. The technique is based on the use of a double laser pulse. A strong shock was generated in iron targets precompressed by a first weak shock. The effect of precompression was studied. The experiment was performed at the Laboratoire pour l'Utilisation des Lasers Intenses laboratory.

DOI: 10.1103/PhysRevE.70.045401

PACS number(s): 52.50.Lp, 62.50.+p, 91.60.Fe

The equation of state (EOS) of highly compressed matter is of fundamental interest to several branches of physics, including astrophysics, geophysics, and inertial confinement fusion (ICF). So far, only high power lasers have been capable of driving multimegabar shock (up to hundreds of Mbar) and reproducing in the laboratory the same physical conditions as those existing at the interiors of planets. During the last decade, the possibility of producing very high quality laser shocks (either by direct or indirect drive) and using them to perform accurate EOS measurements [1–6] has been demonstrated. However, such experiments only allowed data along the principal Hugoniot curve to be obtained. Although measuring laser Hugoniot states has been a very significant advance, it is quite restrictive since data over a broader region are needed to give a complete description of materials EOS, including their phase transitions. In particular it would be very interesting to reach unknown regions of the EOS surface such as the melting regions at high pressures or to study EOS along the planetary isentropes. For example, the knowledge of iron phase change at $P > 1$ Mbar has important implications in describing the Earth's core [7]. For instance, the inner core boundary (ICB) is determined by the fusion temperature of iron at pressure of a few Mbar and, until now, the ICB temperature has always been obtained by extrapolations from the fusion temperature measured on the Hugoniot curve. This would make it possible to estimate the amount of heat stored in the core, which is fundamental for the modeling of the convection process in the mantle. Several theoretical and numerical models as well as static diamond anvil and shock experiments [8–11] have contributed to the mapping of the iron phase diagram. However, a coherence of the results has not been reached yet and the bulk properties of iron at such extreme conditions remain uncertain.

In the case of laser driven experiments, several methods have been envisaged to get off-Hugoniot-curve states.

(a) By generating a shock into a porous material [12–14] (i.e., a material that at room temperature and at atmospheric pressure is characterized by a lower density than the standard one). In this way, "exotic" states of matter can be reached, quite far from the states on the standard Hugoniot curve, characterized by higher temperatures at densities lower than the solid density [15].

(b) By generating a shock into a target with an optical window on the rear side. When the shock crosses the interface, a shock is transmitted to the optical window and a rarefaction isentropic wave is reflected into the target. If the optical window remains transparent under compression, it is possible to measure the optical properties and the velocity of the material and/or window interface and therefore to study the unloading isentrope [16].

(c) By generating a shock into a precompressed target. Indeed the target can be compressed isothermally by a static method (e.g., a diamond anvil cell) before a laser-driven shock is launched. By varying the initial density of the sample through the precompression, it is possible to obtain data off the principal Hugoniot curve, accessing conditions unreachable by either static or single shock compression. That is, precompression allows an investigation of the pressure-volume-temperature space between the isentrope and Hugoniot curve [17].

In this paper, we present the feasibility of a fourth method that is based on a multiple shock technique. Here, the precompression is achieved not by using static compression means but by generating a first weak shock into the target. In this way, we get a much stronger precompression and heating

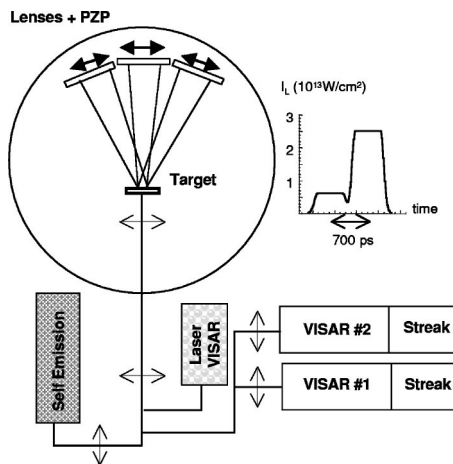


FIG. 1. Experimental setup and temporal shape of the laser pulse used to produce the double shock.

(compared to the static method). A second strong shock is launched 700 ps after the first one to further compress the target. We recall here that multiple shock techniques are of interest not only for the study of EOS regions off the principal Hugoniot curve, but also in the context of ICF research, where they are of primary importance in achieving high gain as they make it possible to minimize the entropy increase (and then the temperature) during the compression [18]. In order to demonstrate that the method works, we compared EOS results obtained at the same compression strength in the case of a single shock and in the case of a double shock.

The experiment was performed at the Laboratoire pour l'Utilisation des Lasers Intenses (LULI) of the Ecole Polytechnique, using three of the six available beams of the LULI Nd-glass laser (converted at $\lambda=0.527 \mu\text{m}$, with a maximum total energy $E_{2\omega} \approx 100 \text{ J}$) focused on a same focal spot. The laser temporal profile was a square with a rise time of 140 ps giving a full width at half maximum (FWHM) of 600 ps. Each beam had a 90 mm diameter and was focused with a 500 mm lens. To eliminate large scale spatial modulations of intensity and to obtain a flat intensity profile in the focal spot [2], we used phase zone plates (PZP) [19]. Characteristics of our optical system (lens+PZP) were such that our focal spot had a 500 μm FWHM, with $a \approx 250 \mu\text{m}$ diameter flat region at the center. To generate a double shock we temporally advanced one of the three laser beams, to have a first pulse characterized by a low intensity [$(6-7) \times 10^{12} \text{ W/cm}^2$] followed after 700 ps by a second one more intense (up to $5 \times 10^{13} \text{ W/cm}^2$). The resulting laser pulse and the experimental set up are showed on Fig. 1.

The principal diagnostic was based on two Velocity Interferometer Systems for any Reflector (VISAR) [20] which allowed us to determine the rear free surface velocity V . Since expected velocities V were of the order of 3–21 km/s, we chose VISARs with 3 mm and 15 mm etalons, giving sensitivities of 16.68 and 3.39 km/(s \times fringe) respectively. The targets were iron planar foils with a thickness of 14 μm .

In the case of a single shock, by measuring the free surface velocity V , we found the fluid velocity U by taking into account that for iron in this range of pressures $V \approx 2U$. Then by using the SESAME tables we obtained all physical quanti-

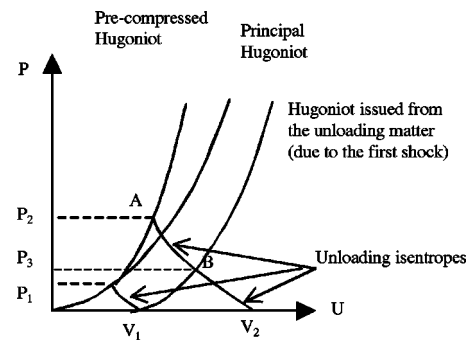


FIG. 2. Representation on the (P, U) plane of the double shock method. P_1 and P_2 are the first and second shock pressure, respectively, and V_1 and V_2 are the free surface velocities experimentally determined with the VISAR interferometers.

ties related to the shock (pressure, density, and internal energy).

In the case of a double shock, we could measure two free surface velocity V_1 and V_2 at successive times due to the two laser pulses. The first low intensity pulse ($6-7 \times 10^{12} \text{ W/cm}^2$) generated a weak shock, which broke out first from the rear surface. Then, as explained above, we could measure V_1 and deduce all parameters associated to the first weak shock. The second high-intensity pulse (up to $5 \times 10^{13} \text{ W/cm}^2$) generated a much stronger shock into a pre-compressed matter. By measuring V_2 , the free surface velocity associated to the second shock breakout, and by knowing the initial conditions given by the first shock, we could obtain pressure, density, and internal energy of the sample after the second compression.

On Fig. 2 we show all the processes on the plane (P, U) . Note that P_3 represents the second shock transmitted into the unloading matter (created by the first one); since the rarefactions waves are isentropic processes [15], the curves issued from the point A and from the point B coincide.

We had also a self-emission diagnostic which was based on a streak camera recording the emitted visible light from the rear surface of the target.

As a first step, we performed a series of shots with a single shock by varying the laser energy. It has been experimentally proved that for iron a shock up to 2–3 Mbar can be considered as a weak shock, imparting an energy to the solid which is not sufficient to vaporize it. In this case when the shock breaks out the free surface is still in solid (or liquid) phase and then it remains a good reflector. Consequently the free surface velocity can be determined with a good precision and for a long time (a few nanoseconds) by the VISARs. In the case of a strong shock ($P > 3 \text{ Mbar}$), the free surface velocity can be measured but only on a shorter time after the shock break out. Indeed we observe the fringe displacement at the shock breakout (for $\approx 100-200 \text{ ps}$ typically) and after this time, the probe beam is completely absorbed by the unloading plasma. The free surface velocities have been measured by the VISAR interferometers and have been compared with the one-dimensional (1D) hydrodynamical simulations. Results are presented in Fig. 3 and show a good agreement.

On the right of Fig. 4 we show a typical VISAR image

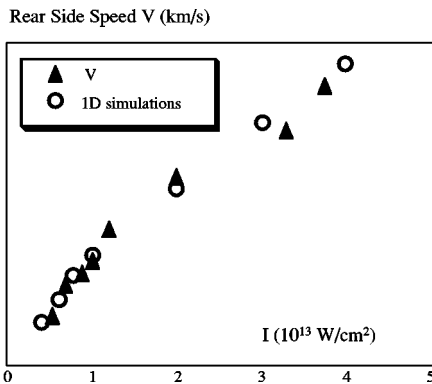


FIG. 3. Triangles: Experimental free surface velocities obtained with a single shock as a function of the laser intensities. Circles: 1D hydrodynamical simulations

obtained with a double shock (on the right) and with a single shock (on the left); the laser intensity in the main compression pulse was the same in the two cases. The front shock curvature on the double shock image is due to the focal spot quality.

In the case of the double shock the laser intensity of the first pulse was 7×10^{12} W/cm² and of the second one was 2.5×10^{13} W/cm². The free surface velocity obtained by the analysis of this image is shown on Fig. 5 and is compared with the 1D simulation. We find a good agreement with simulations on the free surface velocity V_1 associated with the first shock. To reproduce, with simulations, the free surface velocity V_2 associated with the second shock (and also the interval time between V_1 and V_2) we had to adjust the numerical intensity of the second pulse to 2.1×10^{13} W/cm², (i.e., we reduce the intensity by 15%). This low reduction is reasonably due to two different effects that simulations do not take into account. First, the second pulse arrives 700 ps after the first one, so it propagates through an expanding coronal plasma. In this situation, parametric instabilities could play a role into the laser energy deposition. Second, we are probably into a situation where two-dimensional (2D) hydro effects could be not completely negligible.

Figure 6 shows our results in the (P, T) plane obtained by measuring the free surface velocities and by using the SESAME equation of state. Iron is a material that heats up very little when compressed by a shock; consequently our

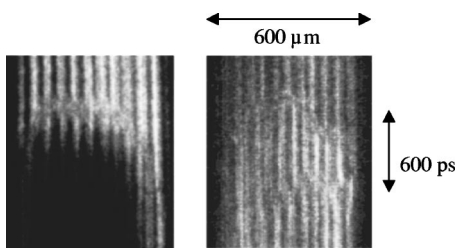


FIG. 4. Experimental images obtained with the VISAR. On the left: the image obtained in the case of a single shock. On the right: the image obtained in the case of a double shock. The laser intensity was the same in both cases.

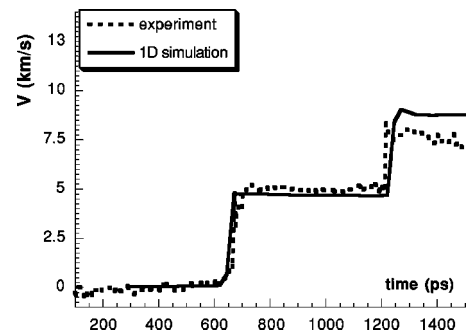


FIG. 5. The free surface velocity in the case of a double shock as function of time compared with the 1D hydrodynamical simulation.

self-emission diagnostic was not sensible enough to get reliable information on temperature. The error bars have been evaluated by considering experimental uncertainty on V of about $\pm 7\%$, which implies an error on pressure and temperature of about $\pm 15\%$. We can notice that at the same pressure (i.e., at the same laser intensity $\approx 2 \times 10^{13}$ W/cm²) in the case of a double shock, the heating of matter was considerably smaller as compared to a single shock. Hence iron is still in its solid phase, unlike in the case of single shock where it is in the liquid phase (according to phase diagram shown in Fig. 6). A clear confirmation of this is given by the reflectivity of the free surface. In the case of the single shock (see Fig. 4 on the left) we observe quite a strong decreasing of the reflectivity after ≈ 300 ps from the shock breakout, due probably to the absorption on the unloading plasma, whereas in the case of the double shock, the reflectivity remains high, even after the second shock breaks out. This is a

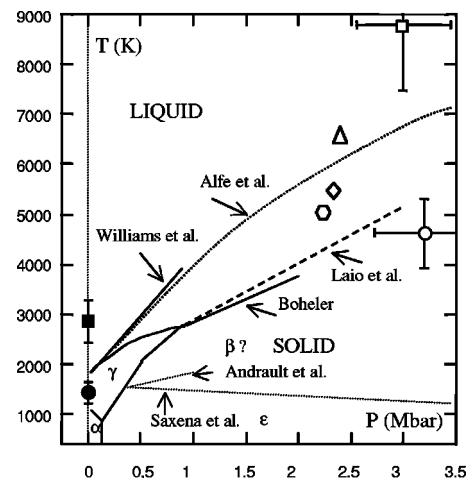


FIG. 6. Iron phase diagram. Solid lines: phase boundaries and melt lines from DAC experiments [8,26]. Dashed lines: *ab initio* calculations [9,27]. Dotted line: possible *b-e* phase boundary [28,29]. The triangle data point is from Yoo *et al.* [16]. Diamond and hexagon data are from the sound velocity experiments by Brown and McQueen [11] and Nguyen and Holmes [30], respectively. Circle data are from the double shock technique: under compression (open circles) and on an unloading wave (plane circle). Squared data are from simple shock: under compression (open squared) and on an unloading wave (plane squared).

clear sign that the state reached with a double shock is denser and colder than the state reached with a single shock. By using again the SESAME tables to calculate isentrope unloading waves and our measurements, we obtained the two points at $P \approx 0$ shown on Fig. 6. The choice of using SESAME tables is supported by the large number of results existing in the literature [21–24]. For example, our previous absolute EOS measurements [24] were in good agreement (within a few percent in the regime $P < 4$ Mbar) with previous experimental results and SESAME tables. So we can affirm that SESAME tables give reliable pressure values in this regime. On the contrary, temperature is more uncertain, since it is the parameter on which the discrepancy between currently available EOS models [9,25] is the most important and for which there is a lack of reliable experimental measurements. Consequently, we tried to deduce temperature values by using other theoretical models [9]. We did not find a significant difference in the sense that our points are always found on either side of the fusion region.

To summarize, we showed the possibility of using a double shock method to get off-Hugoniot-curve states and to

tend towards isentropic compression. Actually, a quasi-isentropic compression is the big challenge for EOS experiments to reproduce interiors of planets and more in general for ICF research. The method presented here opens interesting perspectives for the future.

First, by using stepped targets and then by determining the shock velocity, it should be possible to measure the pre-compressed Hugoniot curve. Compared to static precompression (for iron, by using a digital-to-analog converter, it should be possible to have a precompression of 10 Gpa at the most) this method allows one to investigate a much broader EOS region.

Second, if we apply the same method to iron targets with a transparent window on the rear side to avoid the release into the vacuum (hence states with $P \approx 0$), it is possible to optically have access to the fusion at the ICB conditions.

The authors would like to thank Ph. Moreau (LULI) for his fundamental contribution to the success of the experiment.

-
- [1] T. Löwer *et al.*, Phys. Rev. Lett. **72**, 3186 (1994).
 - [2] M. Koenig *et al.*, Phys. Rev. E **50**, R3314 (1994).
 - [3] M. Koenig *et al.*, Phys. Rev. Lett. **74**, 2260 (1995).
 - [4] L. D. Silva *et al.*, Phys. Rev. Lett. **78**, 483 (1997).
 - [5] A. M. Evans *et al.*, Laser Part. Beams **14**, 113 (1996).
 - [6] R. Cauble *et al.*, Phys. Rev. Lett. **80**, 1248 (1998).
 - [7] W. Anderson and T. Ahrens, J. Geophys. Res. **99**, 4273 (1994).
 - [8] R. Boehler, Nature (London) **363**, 534 (1993).
 - [9] A. Laio *et al.*, Science **287**, 1027 (2000).
 - [10] C. S. Yoo *et al.*, Science **270**, 1473 (1995).
 - [11] J. M. Brown and R. G. McQueen, J. Geophys. Res. **91**, 7485 (1986).
 - [12] N. Holmes, Rev. Sci. Instrum. **62**, 1990 (1991).
 - [13] M. Koenig *et al.*, Phys. Plasmas **6**, 3296 (1999).
 - [14] R. F. Trunin *et al.*, Sov. Phys. JETP **69**, 580 (1989).
 - [15] Y. B. Zeldovich and Y. P. Raizer, *Physics of Shock Waves and High Temperature Hydrodynamic Phenomena* (Academic Press, New York, 1967).
 - [16] C. S. Yoo, N. C. Holmes, and M. Ross, Phys. Rev. Lett. **70**, 3931 (1993).
 - [17] K. M. Lee *et al.*, in *Shock Compression of Condensed Matter*, edited by M. D. Furnish, N. D. Thadhani, and Y. Horie, AIP Conf. Proc. No. 620 (AIP, Melville, 2002), p. 1363.
 - [18] J. Lindl, Phys. Plasmas **2**, 3933 (1995).
 - [19] T. H. Bett *et al.*, Appl. Opt. **34**, 4025 (1995).
 - [20] P. M. Celliers *et al.*, Appl. Phys. Lett. **73**, 1320 (1998).
 - [21] K. K. Krupnikov *et al.*, Sov. Phys. Dokl. **8**, 205 (1963).
 - [22] L. V. Al'tshuler *et al.*, Sov. Phys. JETP **7**, 606 (1958).
 - [23] R. F. Trunin *et al.*, Sov. Phys. JETP **75**(4), 777 (1992).
 - [24] A. Benuzzi-Mounaix *et al.*, Phys. Plasmas **9**, 2466 (2002).
 - [25] R. M. More *et al.*, Phys. Fluids **31**, 3059 (1988).
 - [26] Q. Williams, E. Knittle, and R. Jeanloz, J. Geophys. Res. **96**, 2171 (1991).
 - [27] D. Alfé, M. J. Gillian, and G. D. Price, Nature (London) **401**, 462 (1999).
 - [28] S. Saxena and L. S. Dubrovinsky, Am. Mineral. **85**, 372 (2000).
 - [29] D. Andrault *et al.*, Am. Mineral. **85**, 364 (2000).
 - [30] J. H. Nguyen and N. C. Holmes, Nature (London) **427**, 339 (2004).